A method for computing ion energy and angular distributions for multiple ion species in a collisionless rf sheath

D. C. Kwon, M. Y. Song, and J.-S. Yoon

Plasma Technology Research Center, Daejeon, Korea

In plasma etching system which have radio frequency (rf) biased on a substrate, the rf sheath must be accurately represented to properly simulate the ambipolar fields, electron stochastic heating, and a self-bias. Accordingly, many research groups have been researching the rf sheath by using the numerical, analytic, and semi-analytic models [1-10]. In particular, electronegative plasmas, which are composed of electronegative partially ionized gases, are commonly used in plasma processing reactors [11]. For electronegative plasmas, Dai *et al.* [12] obtained the IEDs at rf-biased electrodes in fluorocarbon plasmas by using an one-dimensional multiple ion dynamics model. The spatiotemporal variations of different species ion densities, the sheath voltage drop, and the sheath thickness are calculated by including all time-dependent terms in the ion fluid equations. The authors of Ref. [12] shown that the sheath structure is different from those of single-ion species plasmas and multiple peaks appear in the ion energy distributions due to the existence of multi-ion species. However, numerically resolving the microscale thin sheath in macroscale computer models of the plasma devices requires large computing resources. Moreover, although Alterkop [13] proposed the electrostatic sheath criterion for both electropositive and electronegative plasmas,

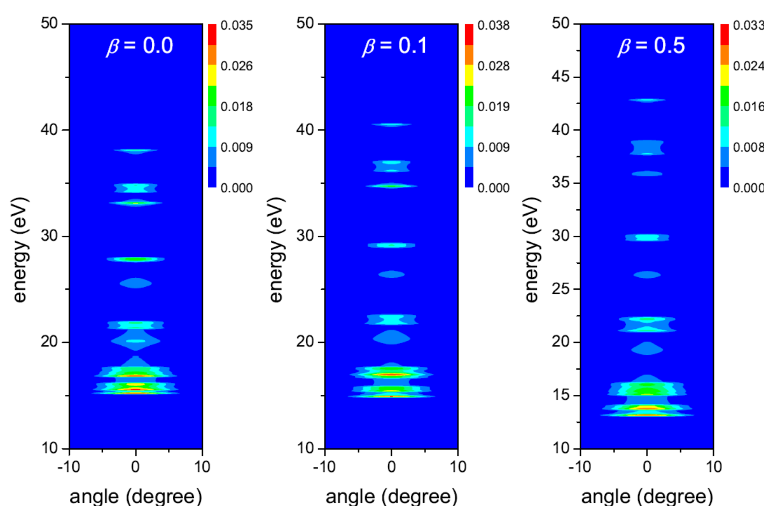

Fig. 1. Dependence of Ion energy and angle distributions for CF_3^+ species on β.

Table 1. The default plasma parameters in the computations.

parameters	value	units
Ar^+	$0.5 \times n_0$	m^{-3}
CF^+	$0.1 \times n_0$	m^{-3}
CF_2^+	$0.1 \times n_0$	m^{-3}
CF_3^+	$0.3 \times n_0$	m^{-3}
CF^-	$\beta \times n_0$	m^{-3}

the electrostatic sheath criterion has not been extended for rf-biased electrodes.

Therefore, we recently extended previous semi-analytic models for a collisionless rf biased sheath in electronegative plasmas [14]. The extended model was based on the previously developed models and an equivalent circuit model to determine the plasma potential and the potential drop within the sheath region. Using the obtained sheath characteristics, we investigated ion energy and angular distributions (IEADs) in the collisionless rf sheath.

In this work, we obtained IEADs based on the semi-analytic sheath model for electronegative plasmas. The defaults plasma parameters used in these calculations are summarized in Table 1 where $\beta = 0.1$ and $n_0 = 3\times10^{16}\ m^{-3}$. And the chamber and the external parameters are set to $R_p = 0.25\ m$, $L_p = 0.1\ m$, $R_{sub} = 0.18\ m$, $C_{LF}^b = C_{HF}^b = 1500$ pF, $V_{LF}^{\max} = 200\ V$, $V_{HF}^{\max} = 50\ V$, $\omega_{LF}/2\pi = 5\ MHz$, $\omega_{HF}/2\pi = 50\ MHz$, $T_e = 3$ eV, and $T_i = 0.1$ eV. Here, '*LF*' and '*HF*' denote the lower and higher frequencies, respectively.

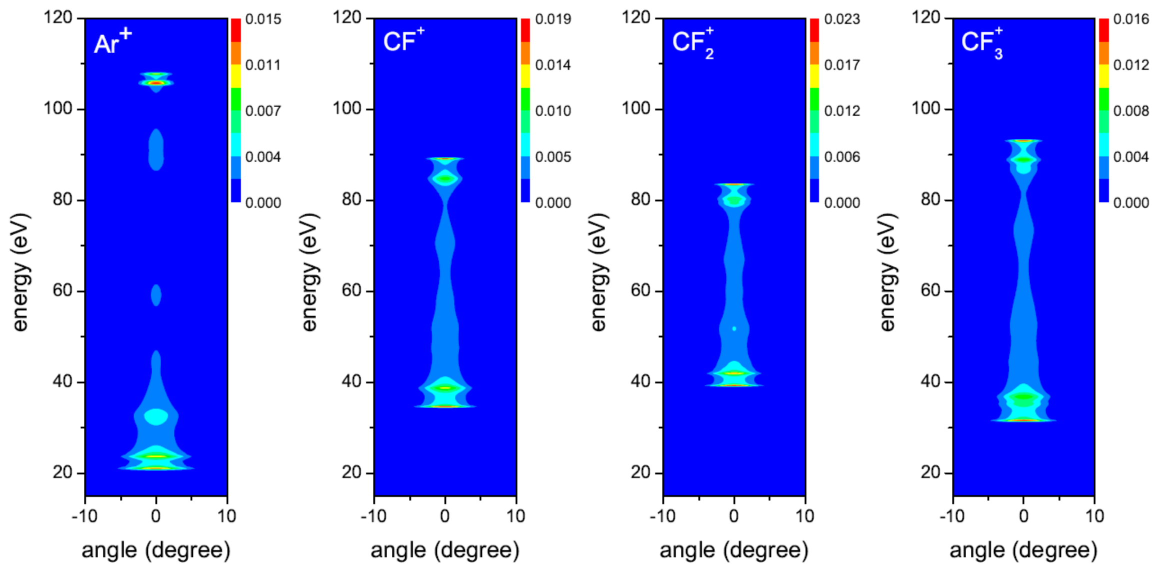

Fig. 2. Ion energy and angular distributions at $n_0 = 5\times10^{16}\ m^{-3}$.

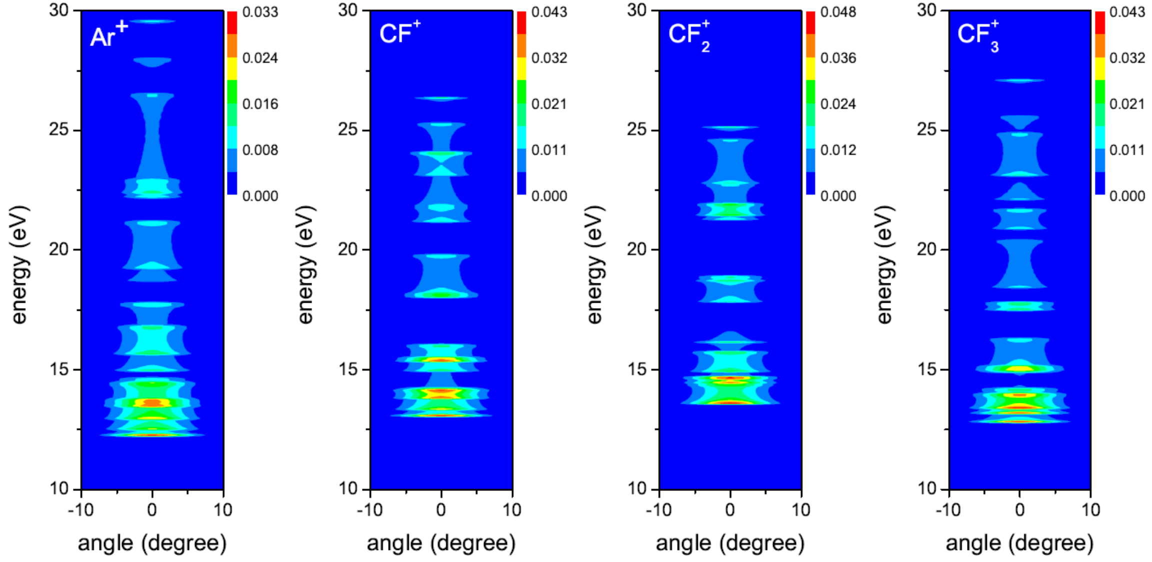

Fig. 3. Ion energy and angular distributions at $n_0 = 5\times10^{17}\ m^{-3}$.

In Fig. 1, dependence of the IEADs for CF_3^+ species on β is shown. The IEADs were calculated using the temporal damped potentials and an analytic model for evaluation of ion angular distribution functions (IADs) [15]. Firstly, the IEDs on the substrate were obtained by using the below formula

$$\mathrm{IEDs}(E_i) \propto \sum_j \left| \frac{d\overline{V}_{s,i}}{dt_j} \right|^{-1} \tag{1}$$

where j is the energy interval and E_i is the ion energy at the substrate [7,16]. After calculating the IEDs, then we can evaluate the IADs as

$$\mathrm{IADs}(\theta) \propto \frac{1}{\cos^2\theta} \exp\left[-\frac{m_i}{2k_B T_i} \upsilon_{i,s}^2 \tan^2\theta \right] \tag{2}$$

where θ is a polar angle and $\upsilon_{i,s}^2 = 2E_i/m_i$ [15]. Magnitudes of the IADs are set to the values of the IEDs at each energy point, i.e. the IADs are normalized with the IEDs. Finally, after normalizing the IEADs with $\iint \mathrm{IEADs}(E_i,\theta)dE_i d\theta$, we can obtain the normalized IEADs for collision less rf sheath model at the substrate. In Ref. [17], a simplified Monte Carlo model of the collisionless ion transport across the sheath was used to calculate the IADs striking the electrode. However, in this work, we directly obtained the IEADs using the above method. We can see that the energy dispersion increases as β increases. At $\beta = 0.1$, the number of high energy ions is slightly increased, but the distribution of lower energy regime is about the same comparing with the condition at $\beta = 0$. However, at $\beta = 0.5$, not only the

number of high energy ions is increased, but also the number of low energy ions is decreased slightly. As mentioned in the preceding text, although negative ion densities are almost zero within the sheath because the thermal velocity of negative ion species is very small, negative ion species can affect the characteristics of rf sheaths.

Figures 2 and 3 show the IEADs at $n_0 = 5\times10^{16}\ m^{-3}$ and $n_0 = 5\times10^{17}\ m^{-3}$, respectively. We can see that the high energy peak position of the IEDs is shifted to the lower energy region and the energy dispersion decreases as the plasma density increases. These results are qualitatively similar as reported in Ref. [12].

In summary, we applied the previously developed model to the dual frequency rf biased electrodes. Using the obtained sheath characteristics, we investigated IEADs in the collisionless rf sheath. We observed that negative ion species could affect the characteristics of rf sheaths, hence negative ion species should be considered to obtain the more accurate IEADs. However, densities at the sheath edge were not determined with self-consistent manner. In particular, the negative ion density at the sheath edge is accurately calculated for highly negative plasmas. Therefore, we will determine the ion densities with coupling the transport model in a self-consistent manner, this is under active study and will be reported late.

References

[1] A. Metze, D. W. Ernie, and H. J. Oskam, J. Appl. Phys. **60**, 3081 (1986).

[2] M. A. Lieberman, IEEE Trans. Plasma Sci. **16**, 638 (1988).

[3] M. A. Lieberman, IEEE Trans. Plasma Sci. **17**, 338 (1989).

[4] V. A. Godyak and N. Stenberg, IEEE Trans. Plasma Sci. **18**, 159 (1990).

[5] V. A. Godyak and N. Stenberg, Phys. Rev. A **42**, 2299 (1990).

[6] P. A. Miller and M. E. Riley, J. Appl. Phys. **82**, 3689 (1997).

[7] T. Panagopoulos and D. J. Economou, J. Appl. Phys. **85**, 3435 (1999).

[8] E. A. Edelberg and E. S. Aydil, J. Appl. Phys. **86**, 4799 (1999).

[9] D. Bose, T. R. Govindan and M. Meyyappan, J. Appl. Phys. **87**, 7176 (2000).

[10] Z. L. Dai, Y. N. Wang and T. C. Ma, Phys. Rev. E **65**, 036403 (2002).

[11] J. I. Fernandez Palop, J. Ballesteros, R. M. Crespo, and M. A. Hernandez, J. Phys. D: Appl. Phys. **41**, 235201 (2008).

[12] Z. L. Dai and Y. N. Wang, Phys. Rev. E **66**, 026413 (2002).

[13] B. Alterkop, J. Appl. Phys. **104**, 123301 (2008).

[14] D. C. Kwon, H. U. Chang, and J.-S. Yoon, 64th Gaseous Electronics Conference (2011).

[15] L. L. Raja and M. Linne, J. Appl. Phys. **92**, 7032 (2002).

[16] Alan C. F. Wu, M. A. Lieberman, J. P. Verboncoeur, J. Appl. Phys. **101**, 056105 (2007).

[17] Z. L. Liu, X. B. Jing, and K. L. Yao, J. Phys. D: Appl. Phys. **38**, 1899 (2005).